The structure of spider toxin huwentoxin-II with unique disulfide linkage: Evidence for structural evolution

QIN SHU,[1] SHAN-YUN LU,[1] XIAO-CHENG GU,[1] AND SONG-PING LIANG[2]

[1]Life Science College, Peking University, Beijing 100871, People's Republic of China
[2]Life Science College, Hunan Normal University, Changsha 410081, People's Republic of China

(RECEIVED July 24 2001; FINAL REVISION October 12, 2001; ACCEPTED October 26 2001)

Abstract

The three-dimensional structure of huwentoxin-II (HWTX-II), an insecticidal peptide purified from the venom of spider *Selenocosmia huwena* with a unique disulfide bond linkage as I-III, II-V, and IV-VI, has been determined using 2D ^{1}H-NMR. The resulting structure of HWTX-II contains two β-turns (C4-S7 and K24-W27) and a double-stranded antiparallel β-sheet (W27-C29 and C34-K36). Although the C-terminal double-stranded β-sheet cross-linked by two disulfide bonds (II-V and IV-VI in HWTX-II, II-V and III-VI in the ICK molecules) is conserved both in HWTX-II and the ICK molecules, the structure of HWTX-II is unexpected absence of the cystine knot because of its unique disulfide linkage. It suggests that HWTX-II adopts a novel scaffold different from the ICK motif that is adopted by all other spider toxin structures elucidated thus far. Furthermore, the structure of HWTX-II, which conforms to the disulfide-directed β-hairpin (DDH) motif, not only supports the hypothesis that the ICK is a minor elaboration of the more ancestral DDH motif but also suggests that HWTX-II may have evolved from the same structural ancestor.

Keywords: Huwentoxin-II; spider toxin; three-dimensional structure; disulfide bond; inhibitor cystine knot motif; disulfide-directed β-hairpin; two-dimensional NMR

Huwentoxin-II (HWTX-II) is an insecticidal peptide purified from the venom of the spider *Selenocosmia huwena*. It can paralyze cockroaches reversibly for several hours, with an ED_{50} of 127 ± 54 μg/g, and cooperatively potentiates the activity of huwentoxin-I to block the neuromuscular transmission in isolated mouse phrenic nerve diaphragm preparations (Shu and Liang 1999). HWTX-II contains 37 amino acid residues, including six cysteine residues that form three pairs of disulfide bond. Assignment of the three disulfide bonds of HWTX-II reveals a unique linkage pattern as I-III, II-V, and IV-VI (C4-C18, C8-C29, and C23-C34) (Fig. 1) (Shu et al. 2001a).

The reported structures of spider toxins such as ω-agatoxin IVA (Reily et al. 1994; Kim et al. 1995), ω-agatoxin IVB (Yu et al. 1993; Reily et al. 1995), μ-agatoxin I (Omecinsky et al. 1996), ω-atracotoxin-HV1 (Fletcher et al. 1997a), δ-atracotoxin-Hv1b (Fletcher et al. 1997b), robustoxin (Pallaghy et al. 1997), J-ACTX-Hv1c (Wang et al. 2000), huwentoxin-I (Qu et al. 1997), and *S. huwena* lectin-I (Lu et al. 1999) share the same structural scaffold known as the inhibitor cystine knot (ICK) motif (Pallaghy et al. 1994; Norton and Pallaghy 1998). The ICK motif is also adopted by a variety of toxic and inhibitory polypeptides from aquatic cone snails and other sources despite their dissimilar primary sequences and biological functions. The typical characteristic of these structures is the cystine knot formed by three disulfide bonds linked in the mode of I-IV, II-V, and III-VI, in which the III-VI disulfide passes through a

Reprint requests to: Song-Ping Liang, Life Science College, Hunan Normal University, Changsha 410081, People's Republic of China; e-mail: liangsp@public.cs.hu.cn; fax: 86731-8861304.

Abbreviations: HWTX-II, huwentoxin-II; 2D NMR, two dimensional nuclear magnetic resonance; COSY, correlation spectroscopy; DQF-COSY, double-quantum-filtered COSY; NOESY, nuclear Overhauser effect spectroscopy; TOCSY, total correlated spectroscopy; NOE, nuclear Overhauser effect; RMS, root mean square; ICK, inhibitor cystine knot, DDH, disulfide-directed β-hairpin.

Article and publication are at http://www.proteinscience.org/cgi/doi/10.1110/ps.30502.

Fig. 1. Comparison of disulfide bond linkage pattern of huwentoxin-II, huwentoxin-I, ω-agatoxin IVA, δ-atracotoxin-Hv1b, and J-atracotoxin Hv1c. Huwentoxin-II has a unique disulfide-pairing mode as I-III, II-V, and IV-VI. Huwentoxin-I, ω-agatoxin IVA, δ-atracotoxin-Hv1b, and J-atracotoxin Hv1c represent four kinds of disulfide pairing modes found in spider toxins that adopt the inhibitor cystine knot motif in three-dimensional structures.

ring consisting of a minimum of 10 residues formed by the I-IV and II-V disulfide bonds and the intervening polypeptide backbone.

It is also found that only the II-V disulfide is conserved both in HWTX-II and the ICK folding molecules from the primary sequence comparison. Because of the importance of disulfide bridges in the structures of small, highly cross-linked peptides, the unique disulfide-bonding mode (I-III, II-V, and IV-VI) of HWTX-II implies that the three-dimensional structure of HWX-II might be unusual. To investigate the structural features and elucidate the structure-function relationship of HWTX-II, its solution structure is determined by 2D ^{1}H- NMR.

The three-dimensional structure of HWTX-II demonstrates a fold different from the ICK motif found earlier in spider toxins and provides new insights into the evolution of structural motifs.

Results

Sequence-specific resonance assignments were performed following the standard method (Wüthrich et al. 1986). All of the backbone protons and side chain protons except the εNH_2 of Lys were identified in our previous paper (Shu et al. 2001b). The three-dimensional structure of HWTX-II was calculated using the program X-PLOR (Brünger 1992). A total of 592 non-redundant interproton distance constraints and 16 dihedral constraints were used by distance geometry algorithm to obtain 50 initial structures. The initial structures were refined by five rounds of simulated annealing with force constants 50 kcal/mole per Å^2 and 200 kcal/mole per rad^2 for NOE distance and dihedral angle constraints, respectively. The structures with lower energy and better Ramachandran plots were chosen for further refinement. A total of 47 structures agreeing with the experimental constraints were obtained, which converged to a common fold. A total of 10 structures with lower energy and better PROCHECK (Laskowski et al. 1993) results were chosen from the 47 to represent the solution structure of HWTX-II (Fig. 2A). In the family of 10 chosen structures, all NOE violations are <0.3 Å and dihedral violations <2°. The 10 structures exhibit no significant deviation from ideal covalent geometry, satisfy the experiment constraints with minimal violations, and have good non-bonded contacts as evidenced by the low values of the mean Lennard-Jones potential (Table 1). The root mean square differences of these structures are 0.61 ± 0.11 Å over backbone atoms and 1.22 ± 0.13 Å over all heavy atoms, respectively, versus the average structure. The average pairwise RMSD of the 10 structures are 0.91 ± 0.15 Å over backbone atoms and 1.79 ± 0.18 Å over all heavy atoms, respectively. Analysis of the family of 10 structures using Program PROCHECK reveals that 83.5% of all residues lie in the most favored regions of the Ramachandran plot and the remaining 16.5% lie in the additionally allowed regions.

The coordinates for the family of 10 structures and NMR constraints file have been deposited in the Brookhaven Protein Data Bank (PDB) with accession code 1I25. The ^{1}H chemical shifts have been deposited in BioMagResBank (BMRB) with accession code 4988.

Discussion

Secondary structure

The calculated structure of HWTX-II has no helix and contains two β-turns (C4-S7 and K24-W27) and a double-stranded antiparallel β-sheet (W27-C29 and C34-K36). The

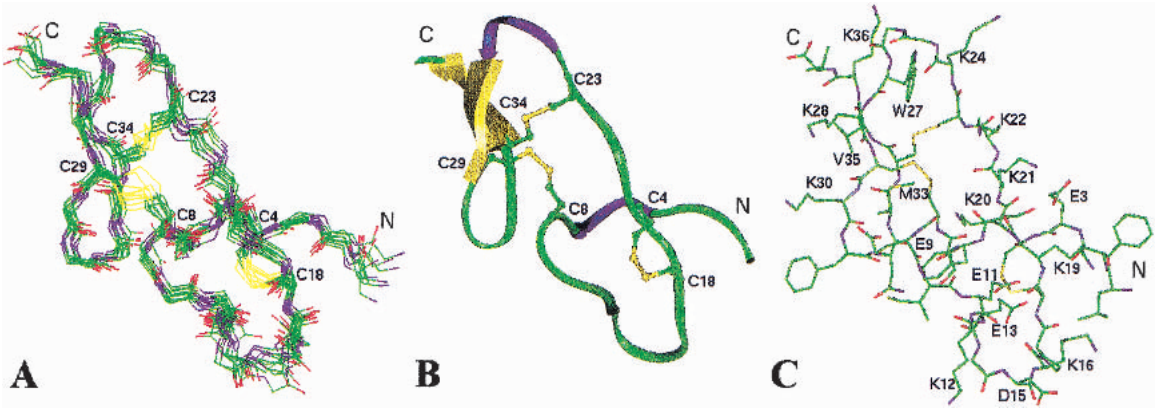

Fig. 2. Three-dimensional solution structure of HWTX-II. (*A*) The backbone atom superimposition plot for the ensemble of 10 HWTX-II structures. The side chain heavy atoms of the disulfide bonds are shown. (*B*) The secondary topology of HWTX-II. The double-stranded antiparallel β-sheet is shown in yellow, and turns in blue, random coil structure is shown in green. The three disulfide bonds (C4-C18, C8-C29, and C23-C34) are indicated. The three-dimensional structure of HWTX-II consists of the N- and C-terminal parts and two connecting elements (the fragment 19–22 and the disulfide C8-C29). (*C*) The charged residues in HWTX-II form a dipolar distribution, and the side chains of residue W27, M33, and V35 distributed around the disulfides C8-C29 and C23-C34 form hydrophobic patches. Both in *A* and *C*, the colors of the C, N, O, and S atom are green, blue, red, and yellow, respectively.

ensemble of 10 structures of HWTX-II was analyzed using InsightII (Biosym Technologies). The double-stranded antiparallel β-sheet at the C terminal and the hydrogen bonds of HN(V37)-O(G26), HN(K28)-O(V35), O(K28)-HN(V35), and HN(K30)-O(M33) are found in the 10 structures. Long-distance NOE connections were observed between fragment 3–4 and 18–20, and the hydrogen bonds of HN(C4)-O(K19) and O(F2)-HN(K19) exist in 7 of the 10 structures analyzed by InsightII. It shows that fragments 2–4 and 18–20 are in close vicinity to each other that may be related to the disulfide linkage of C4-C18.

Table 1. *Structural statistics for the family of 10 structures of HWTX-II*

	Number
Experiment constraints	
Intra-residue NOE (|i − j| = 0)	179
Sequential NOE (|i − j| = 1)	212
Medium-range NOE (|i − j| ≤ 5)	57
Long-range NOE (|i − j| ≥ 5)	144
Dihedral angle	16
RMS deviation from experimental constraints[a]	
NOE distance (Å) (592)	0.002 ± 0.001
Dihedral angle (deg.) (16)	0.194 ± 0.141
RMS deviations from idealized geometry[b]	
Bonds (Å)	0.0029 ± 0.0002
Angles (deg)	0.5055 ± 0.0055
Impropers (deg)	0.3332 ± 0.005
Mean energies (kcal mol^{-1})[b]	
E_{bond}	5.22 ± 0.53
E_{angle}	43.21 ± 0.93
$E_{improper}$	5.12 ± 0.15
E_{vdW}	−112.77 ± 7.28
E_{NOE}	0.17 ± 0.16
E_{cdih}	0.05 ± 0.05

[a] The statistics of experimental RMS deviation of NOE and dihedral angle constraints were from the calculation with force constants of 50 kcal mol^{-1} $Å^{-2}$ and 200 kcal mol^{-1} rad^{-2}, respectively.
[b] The idealized geometry and energy values were defined by the CHARMM force field as implemented in XPLOR program. All statistical values of energies, RMS deviations, and RMS differences are given as the mean ± S.D. (standard deviation).

Both average distance between $C^{\alpha}(i)$ and $C^{\alpha}(i+3)$ of loop 4–7 and 24–27 are less than 7Å and form the type I β-turn. For loop 4–7, the average ϕ, ψ torsion angles for S5 and F6 are −93°, −24°, and −101°, −26°, respectively. The average ϕ, ψ torsion angles for G25 and G26 in loop 24–27 are −65°, −40° and −90°, 21°, respectively.

Some amide protons are involved in forming the secondary structures in HWTX-II. All hydrogen-bonded amide protons taking part in the secondary structures should be well solvent exposed, as no slow exchanging NH was recorded in the hydrogen-deuterium exchange experiments carried out under the same experimental condition used for the structure determination.

Description of the three-dimensional structure

The molecule of HWTX-II is composed of the N- and C-terminal parts and two connecting elements (the fragment 19–22 and the disulfide C8-C29) between them (Fig. 2B). The N part of the structure consists of the disulfide bond C4-C18 and the peptide backbone from N terminal to residue 18. It contains no regular secondary structure except for a β-turn (loop 4–7). The C part is formed by the disulfide bond C23-C34 and the peptide fragment from the 23rd residue to the C terminus. It contains the double-stranded an-

tiparallel β-sheet (27–29 and 34–36) and a β-turn 24–27. The N and C parts are connected together to form a globular fold because of the extended fragment 19–22 and the disulfide C8-C29. The fragment 19–22 lying between two cysteine residues (C18 and C23) consists of four consecutive positively charged residues (K19, K20, K21, and K22). The disulfide bond C8-C29 should be the important covalent factor contributing to the globular folding of HWTX-II.

Charged residues

The insecticidal toxin HWTX-II contains many charged residues (15 among a total of 37 residues), including 10 alkaline residues (K12, K16, K19-K22, K24, K28, K30, and K36) and 5 acidic residues (E3, E9, E11, E13 and D15). Accordingly, HWTX-II is a positively charged molecule, in accordance with the experimental pI value of 9.2 from the two-dimensional electrophoresis results (Liang et al. 2000). All acidic residues with negatively charged side chains are distributed in the N part of the molecule (Fig. 2C). Among the 10 positively charged residues, 4 are distributed in the connecting fragment residues 19–22 as described formerly, 4 lie in the C part, and only 2 in the N part. This dipolar distribution of charged residues in structure is found not only in HWTX-II but also in other molecules such as the neutral or anionic μ-agatoxin I, which paralyzes insects by modifying the kinetics of neuronal voltage-activated sodium channels (Omecinsky et al. 1996). However, our whole-cell patch clamp recording results prove that HWTX-II shows little effect on the voltage-gated sodium, calcium, and potassium channel current in acutely isolated rat dorsal root ganglion neuron (Q. Shu and S.P. Liang).

Hydrophobic patches

The structure of HWTX-II is not so compact as huwentoxin-I purified from the venom of the same spider *S. huwena* (Fig. 3, cf. A and B). Most residues of HWTX-II are solvent exposed and the molecule lacks a hydrophobic core, because of the loose main chain folding. However, the side chains of residues W27, M33, and V35 are distributed around the two disulfide bonds of C8-C29 and C23-C34 to form more hydrophobic patches on the surface of HWTX-II (Fig. 2C). It is also shown that these residues mostly take part in forming the double-stranded antiparallel β-sheet of the C-terminal part.

Structure comparison

Numerous NMR structures of spider toxins such as ω-agatoxin IVA (Reily et al. 1994; Kim et al. 1995), ω-agatoxin IVB (Yu et al. 1993; Reily et al. 1995), μ-agatoxin I (Omecinsky et al. 1996), ω-atracotoxin-HV1 (Fletcher et al. 1997a), δ-atracotoxin-Hv1b (Fletcher et al. 1997b; Szeto et al. 2000), robustoxin (Pallaghy et al. 1997), J-atracotoxin Hv1c (Wang et al. 2000), hanatoxin1 (Takahashi et al. 2000), heteropodatoxin 2 (Bernard et al. 2000), huwentoxin-I (Qu et al. 1997), and *S. huwena* lectin-I (Lu et al. 1999) and the predicted structure of μ-agatoxin IV (Omecinsky et al. 1996) have been reported. These polypeptides have different biological functions and come from different species of spiders, but their three-dimensional structures all adopt the ICK motif. It is shown that the numbers and linkage modes of disulfide bonds in these polypeptides are different and they can be divided into four categories. First, the normal ICK motif is where the three disulfide bridges are paired in I-IV, II-V, and III-VI mode. ω-atracotoxin HV1(an inhibitor of insect voltage-gated calcium channel currents), hanatoxin1 (a gating modifier of voltage-dependent potassium channels), heteropodatoxin (a blocker of Kv4.2 potassium channel currents), neurotoxin huwentoxin-I, and lectin peptide SHL-I all belong to this category (see Fig. 1). Second, ω-agatoxin IVA and ω-agatoxin IVB (P-type calcium channel blocker), μ-agatoxin I, and μ-agatoxin IV (insecticidal toxin) all contain four disulfide bonds with I-IV, II-V, III-VIII, and VI-VII linkage (see Fig. 1). Third, robustoxin and δ-atracotoxin-Hv1b (versutoxin) are sodium channel modulators, containing four disulfide bonds with I-IV, II-VI, III-VII, and V-VIII linkage (see Fig. 1). Furthermore, the four disulfide bonds of insecticidal neurotoxin J-atracotoxin Hv1c are linked in the pattern of I-VI, II-VII, III-IV, and V-VIII, where the III-IV disulfide (C13-C14) is a vicinal bridge and critical for insecticidal activity (see Fig. 1) (Wang et al. 2000). Four ICK motif spider toxins representing four kinds of different numbers and bonding modes of disulfide bonds, as huwentoxin-I (Fig. 3B), δ-atracotoxin-Hv1b (Fig. 3C), ω-agatoxin IVA (Fig. 3D), and J-atracotoxin Hv1c (Fig. 3E), respectively, are chosen for comparison with HWTX-II (Fig. 3A).

The three-dimensional structures of the four categories of ICK molecules all form the cystine knot although they contain different numbers and linkage modes of disulfide bonds. As shown in Figure 3C–E, the ICK molecules with four disulfide bridges linked in different modes always have three of the four playing similar roles of the three disulfide bonds paired as I-IV, II-V, and III-VI in the typical ICK fold molecule (Fig. 3B) (shown in yellow). The fourth additional disulfide (shown in red) contributes to the stability of special regions such as C16-C42 in δ-atracotoxin-Hv1b (Fig. 3C) and C27-C34 in ω-agatoxin IVA (Fig. 3D) or is related to the biological activity as C13-C14 in J-atracotoxin Hv1c (Fig. 3E). Therefore, the I-IV, II-V, and III-VI disulfide linkage dictated the structural scaffold of ICK motif is further compared with HWTX-II.

Although HWTX-II does not form the cystine knot because of the unique I-III, II-V, and IV-VI disulfide bond-pairing pattern (Fig. 3A), it shows similarities in structure with the ICK motif molecules. The C-terminal parts in all

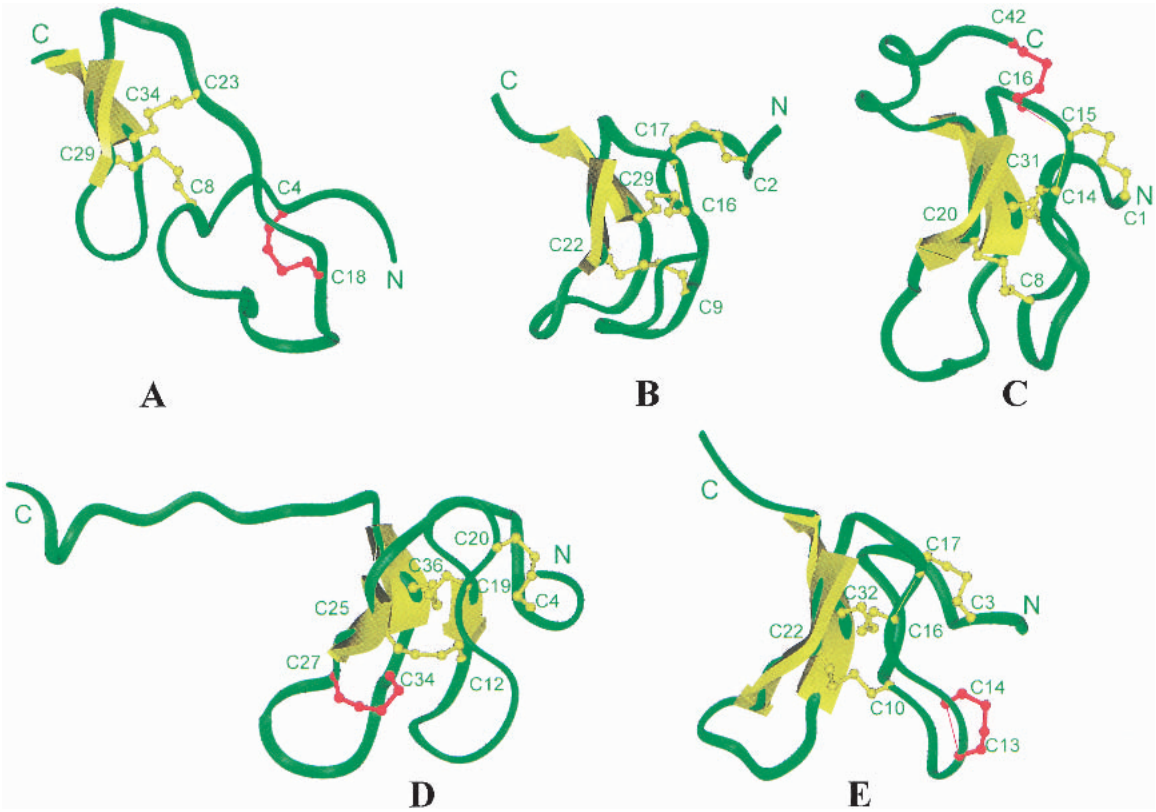

Fig. 3. Comparison between HWTX-II (*A*) and the inhibitor cystine knot motif molecules (*B–E*) with different disulfide bond numbers and linkage patterns. The backbone folding (in green), the sheet structures (in yellow) classified by Kabsch-Sander method in InsightII, and disulfide bonds are shown. (*A*) HWTX-II. Three disulfide bonds link in I-III, II-V, and IV-VI (C4-C18, C8-C29, and C23-C34) mode. (*B*) Huwentoxin-I. Three disulfides shown in yellow are linked in the typical ICK motif mode as I-IV, II-V, and III-VI (C2-C17, C9-C22, and C16-C29) (cf. Fig. 1). The III-VI disulfide passes through a ring formed by the I-IV and II-V disulfide bonds and the intervening peptide backbone, it is known as the cystine knot. (*C*) δ-atracotoxin-Hv1b. Four disulfides linked in C1-C15, C8-C20, C14-C31, and C16-C42 (cf. Fig. 1). (*D*) ω-agatoxin IVA. Four disulfides linked in C4-C20, C12-C25, C19-C36, and C27-C34 (cf. Fig. 1). (*E*) J-atracotoxin Hv1c. Four disulfides linked in C3-C17, C10-C22, C13-C14, and C16-C33 (cf. Fig. 1). The disulfide bonds involving in the cystine knot (I-IV, II-V, and III-VI) in the ICK motif structures, i.e. *B*, *C*, *D*, and *E*, are shown in yellow. The fourth additional disulfides (shown in red in *B–E*) in the ICK folding molecules are various and not involved in the cystine knot such as C16-C42 in δ-atracotoxin-Hv1b (*C*), C27-C34 in ω-agatoxin IVA (*D*), and C13-C14 in J-atracotoxin Hv1c (*E*). The ICK motif spider toxins with different disulfide bond numbers and linkages (*B–E*) all form the cystine knot, whereas HWTX-II (*A*) does not because of its unique disulfide bridges linkage. Moreover, the II-V and the IV-VI disulfide bond of HWTX-II (shown in yellow in *A*) dictating the C-terminal β-hairpin are similar to corresponding ones in ICK folding molecules (*B–E*). The disulfide I-III of HWTX-II (shown in red in *A*) is different from the corresponding ones of ICK folding molecules.

the five structures (Fig. 3A–E), especially the double-stranded antiparallel β-sheet and the correlative two disulfide bridges, are conserved. The disulfide bonds II-V and IV-VI in HWTX-II (shown in yellow in Fig. 3A) are similar to the II-V and III-VI in the ICK motif molecules (Fig. 3B–E), respectively. The significant difference between HWTX-II and the ICK motif molecules is the N-terminal part, which is contributed from the I-III disulfide bond of HWTX-II (shown in red) (see Fig. 3).

Novel structure motif

Because HWTX-II does not form a cystine knot, the structure of HWTX-II may be considered as the first representative of a novel structural scaffold found in spider toxins. Moreover, this fold may also be adopted by other molecules in addition to HWTX-II. The primary structure of HWTX-II (Shu and Liang 1999) is highly homologous with ESTX from the American tarantula spider *Eurypelma californicum* (Anette 1989) and venom protein 1 from the Mexican red knee tarantula spider *Brachypelma smithii* (Kaiser et al. 1994), as shown in Figure 4 (Shu et al. 2001a). The high homology of these three toxins in primary sequence may imply that the molecular folding of ESTX and venom protein 1 could be similar to HWTX-II. The three disulfide bonds of ESTX and venom protein 1 could also be linked in the HWTX-II mode of I-III, II-V, and IV-VI, although they are reported to be I-IV, II-V, and III-VI determined by

Fig. 4. Sequence alignment of HWTX-II, TX4K EURCA from *Eurypelma californicum* and TXP1 BRASM from *Brachypelma smithii*. TX4K EURCA and TXP1 BRASM are the ID numbers of Swissprot database to ESTX and venom protein 1, respectively. Gaps have been inserted to achieve the best alignment. Residues conserved for HWTX-II, ESTX, and venom protein 1 are shaded and residues identical among the three molecules are given against a black background.

similarity in the Swissprot Database (cf. ID number TX4K_EURCA and TXP1_BRASM, respectively). The structure of HWTX-II might serve as a new reference to modeling the three-dimensional structures of ESTX and venom protein 1.

Evidence for structural evolution

It has been shown that the ICK motif molecules are conserved in the C-terminal structure with more variety than in the N-terminal part. Structure analyses of ω-atracotoxin-HV1 and J-atracotoxin Hv1c (Fig. 5A) with ICK folding show that the compact hydrophobic core of the ICK motif is largely composed of the C-terminal two disulfide bonds and the double-stranded β-sheet. The N-terminal disulfide bridge contributing very little to the core structure is thought to be not essential to the formation of the basic ICK fold (Fletcher et al. 1997a; Wang et al. 2000). The three-dimensional structure of J-atracotoxin Hv1c also revealed that its closest structural homolog searched from the PDB was the cellulose binding domain of cellobiohydrolase I (CBD-CBHI) (Fig. 5B) that missed the N-terminal disulfide bridge of the ICK motif. Therefore it was proposed that the ICK fold was a minor elaboration of a simpler ancestral fold—the disulfide-directed β-hairpin (DDH) fold (Wang et al. 2000). The DDH fold differs from the ICK fold in that there are only two mandatory disulfide bridges (the two that form the bulk of the hydrophobic core).

The DDH fold consensus amino acid sequence has been summarized as $CX_{5-19}CX_2$(G or P)$X_2CX_{6-19}C$, where the two disulfides are cross-linked as C_I-C_{III} and C_{II}-C_{IV}, X is any amino acid, the loop 2 (between C_{II} and C_{III}) is generally five residues in length with a central Gly/Pro to ensure a tight turn prior to the first β-strand, and the residue following the Gly/Pro in loop 2 is generally hydrophobic and along with the two disulfides constitutes the mini-hydrophobic core of the protein (Wang et al. 2000). The C-terminal part in HWTX-II (Fig. 5C) highly conforms to the requirements of the DDH motif as regards the positions and the linkage of the two C-terminal disulfide bridges (C8-C29 and C23-C34), the $CX_{14}CX_2$(G)X_2CX_4C sequence, the residue G26, and its followed residue W27 in loop 2.

It has been noted that the amino acid residue number of the loop 3 between C_{III} and C_{IV} in the DDH fold is ranged 6–19, whereas it is 4 in the loop between C29-C34 in HWTX-II. The loop 3 is related to the lengths of the β-hairpin and the loop inserting between two β-strands. A lower limit of four amino acid residues in the loop 3 in the DDH fold should be reasonable to turn the peptide chain for forming the β-hairpin. We also noted that the spaces between half-cystine residues have been summarized as $CX_{3-7}CX_{4-6}CX_{0-5}CX_{1-4}CX_{4-10}C$ in the ICK motif (Pallaghy et al. 1994; Norton and Pallaghy 1998). Because the

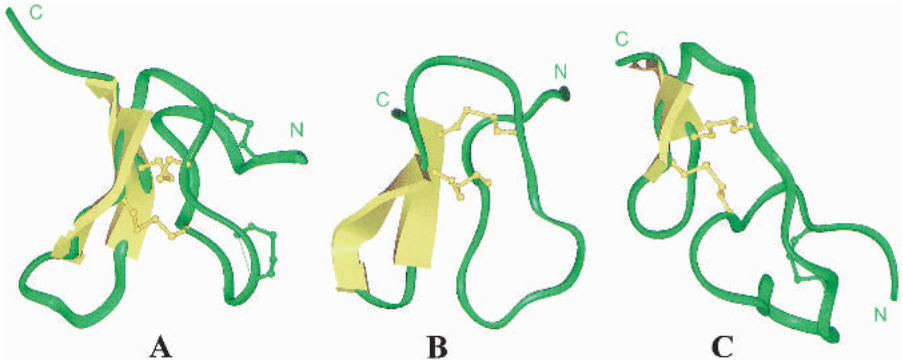

Fig. 5. Comparison of the structure of J-atracotoxin Hv1c, the CBD-CBHI, and HWTX-II. (*A*) J-atracotoxin Hv1c; (*B*) CBD-CBHI; (*C*) HWTX-II. The double-stranded β-sheet dictated by the two cross-linked disulfides in the C-terminal part (shown in yellow) is conserved in three structures.

C-terminal double-stranded β-sheet directed by the II-V and III-VI disulfide bridges in the ICK motif refers to the DDH fold, the amino acid sequence of the ICK motif related to the DDH motif is $CX_{4-6}CX_{2-10}CX_{4-10}C$. As it proposed that the ICK motif is an elaboration of the DDH motif, the upper limit of the amino acid residue number of loop 2 in the DDH fold can be 10 and the lower limit of loop 3 can be 4. It means that the loop 2 and 3 in the DDH fold should be more variable to the sequence $CX_{5-19}CX_2$(G or P)$X_2CX_{6-19}C$ according to the ICK motif, and the loop 3 in HWTX-II also conforms to the DDH fold.

Comparison of the structures of HWTX-II (Fig. 5C) and representatives of the DDH fold such as J-atracotoxin Hv1c (one of the ICK folding molecules) (Fig. 5A) and the CBD-CBHI (Fig. 5B) suggests that HWTX-II may have also evolved from the DDH fold. The structure of HWTX-II might be a molecular evidence for the proposition that the ICK motif was a minor elaboration of the DDH fold. The evolution relationship of HWTX-II, the ICK, the DDH fold, and other structural folds are under further study.

Materials and methods

Sample preparation

HWTX-II was purified from the venom of *S. huwena* by ion exchange chromatography and reverse-phase HPLC as described by Shu and Liang (1999). The purity of the toxin was identified to >95% by N-terminal sequencing and MALDI-TOF mass spectrometry analysis. The sample was prepared by dissolving the lyophilized powder of HWTX-II in 500 μL of 20 mmole/L phosphate buffer (H_2O/D_2O, 9/1, vol/vol), containing 0.002% NaN_3 and 0.1 mmole/L EDTA. The pH value was adjusted to 5.4 by HCl. The final concertration of HWTX-II was 4 mmole/L sodium 3–(trimethyl-silyl)propionate-2,2,3,3-D4 (TSP) and was added to a final concentration of 200 μmole/L as an internal chemical shift reference. For experiments in D_2O, the sample used in the H_2O experiment was lyophilized and redissolved in 500 μL of 99.96% D_2O.

NMR spectroscopy

All NMR experiments were recorded on a 500 MHz Bruker DMX-500 spectrometer. All 2D spectra were recorded in phase-sensitive mode by the time-proportional phase incrementation (TPPI) method following standard pulse sequences and phase cycling. Solvent suppression was achieved by the presaturation method. Homonuclear 2D NMR spectra were recorded at temperature of 300 K, including COSY, DQF-COSY, TOCSY with mixing time of 44 and 85 msec, as well as NOESY with mixing time of 150 200, 250, and 400 msec. The recording data points of t1 × t2 were 512 × 2048 for COSY and TOCSY; 700 × 4096 for DQF-COSY; 512 × 2048 for all NOESY spectra except 768 × 4096 for the 150-msec spectrum. Spectra of NOESY with 400-msec mixing time and TOCSY with 85-msec mixing time were recorded at the temperature of 290 K, the data points of t1 × t2 were 512 × 2048.

Spectra were processed and viewed using software Felix 98.0 (Biosym Technologies) and Sybyl (Tripos) on the O2 workstation (Silicon Graphics). All data were zero-filled to produce a 2K × 4K real matrix to COSY, DQF-COSY and NOESY or 1K × 2K to TOCSY. Before Fourier transformation, sine bell or sine bell square window functions were used with phase shift of $3\pi/4$ or $\pi/2$.

The hydrogen-deuterium exchange experiments were carried out by recording a set of 1D spectra after redissolving the lyophilized H_2O experiment sample in D_2O at time scalar of 10, 20, 30, 60, 90, and 120 min. As no slow exchanging amide proton was observed, no longer time scalar and no 2D experiments were performed.

Structure constraints

Distance constraints were derived primarily from the intensities of cross-peaks in NOESY spectra recorded in H_2O and D_2O with mixing times of 200 msec recorded at 300 K. Comparisons were made to the 150-, 250-, and 400-msec NOESY spectra to assess possible contributions from spin diffusion. All NOE data were classified as strong, medium, or weak, corresponding to upper bound inter-proton distance restraints of 2.7, 3.5, and 5.0 Å, respectively. Lower distance bounds were taken as 1.8 Å, the sum of the van der Waals radii of proton. Pseudo-atom corrections were applied to non-stereo specifically assigned methyl and methylene protons with the upper bound for 0.5 Å (Wüthrich et al. 1986).

Backbone dihedral constraints were inferred from $^3J_{HNH\alpha}$ coupling constants measured from either 1D NMR spectra or the anti-phase cross-peak splitting in a high-digital-resolution DQF-COSY spectrum. 16 ϕ dihedral angles were restrained to $-120 \pm 40°$ for a $^3J_{HNH\alpha} \geq 8$ Hz and $-65 \pm 25°$ for $^3J_{HNH\alpha} \leq 5.5$ Hz.

Nine additional fake distance constraints were added to define the three disulfide bonds involved in HWTX-II. Three distance constraints for each disulfide bond are S(i)-S(j), S(i)-C_β(j), and S(j)-C_β(i), respectively, whose target values were set to 2.02 ± 0.02, 2.99 ± 0.5, and 2.99 ± 0.5 Å, respectively.

Structure calculation and evaluation

The three-dimensional structures were calculated by simulated annealing and energy minimization using the program of X-PLOR (Brünger 1992). A set of 50 structures was calculated as described by Qu et al. (1997). The programs of PROCHECK (Laskowski et al. 1993) were used to assess the overall quality of calculated structures. A family of 10 structures was chosen to represent the solution structure of HWTX-II. The software InsightII (Biosym Technologies) was used to view and plot the structures.

Convergence of the calculated structures was evaluated in terms of the structure parameters, including RMS deviations from experimental distance and dihedral constraints, values of energetic statistics, RMS deviations from idealized geometry, and atomic RMS differences of the family of 10 structures.

Structure comparison

The coordinates of structures used in structural comparison were obtained from the Brookhaven Protein Data Bank. Entry ID of 1OAV is for ω-agatoxin IVA, 1VTX for δ-atracotoxin Hv1b (versutoxin), 1DL0 for J-atracotoxin Hv1c, 1QK6 for huwentoxin-I, and 1AZ6 for CBD-CBHI, respectively.

Acknowledgments

This work was supported by the National "863" Program of China (103–13–01–06). We are grateful to Mr. Renhuai Huang of Hunan

Normal University for providing the sample, to Mr. Mujian Lu of Peking University for collecting the 1D NMR spectrum, and to Professors Yunyu Shi and Jihui Wu for collecting the 2D NMR spectra.

The publication costs of this article were defrayed in part by payment of page charges. This article must therefore be hereby marked "advertisement" in accordance with 18 USC section 1734 solely to indicate this fact.

References

Anette, S.N. 1989. Tarantula (*Eurypelma californicum*) venom, a multicomponent system. *Biol. Chem. Hoppe-Seyler.* **370:** 485–498.

Bernard, C., Legros, C., Ferrat, G., Bishoff, U., Marquardt, A., Pongs, O., and Darbon, H. 2000. Solution structure of hpTX2, a toxin from *Heteropodidae venatoria* spider that blocks KV4.2 potassium channel. *Protein Sci.* **9:** 2059–2067.

Brünger, A.T. 1992. *X-PLOR manual*, Version 3.1. Yale University, New Haven, CT.

Fletcher, J.I., Smith, R., O'Donoghue, S.I., Nilges, M., Connor, M., Howden, M.E., Christie, M.J., and King, G.F. 1997a. The structure of a novel insecticidal neurotoxin, ω-atracotoxin-HV1, from the venom of an Australian funnel web spider. *Nat. Struct. Biol.* **4:**559–566.

Fletcher, J.I., Chapman, B.E., Mackay, J.P., Howden, M.E., and King, G.F. 1997b. The structure of versutoxin (δ-atracotoxin-Hv1) provides insights into the binding of site 3 neurotoxins to the voltage-gated sodium channel. *Structure (London).* **5:** 1525–1535.

Kaiser, I.I., Griffin, P.R., Aird, S.D., Hudiburg, S., Shabanowitz, J., Francis, B., John, T.R., Hunt, D.F., and Odell, G.V. 1994. Primary structures of two proteins from the venom of the Mexican red knee tarantula (*Brachypelma smithii*). *Toxicon* **32:** 1083–1093.

Kim, J.I., Konishi, S., Iwai, H., Kohno, T., Gouda, H., Shimada, I., Sato, K., and Arata, Y. 1995. Three-dimensional solution structure of the calcium channel antagonist ω-agatoxin IVA: Consensus molecular folding of calcium channel blockers. *J. Mol. Biol.* **250:** 659–671.

Laskowski, R.A., MacArthur, M.W., Moss, D.S., and Thornton, J.M. 1993. PROCHECK: A program to check the stereochemical quality of protein structures. *J. Appl. Cryst.* **26:** 283–291.

Liang, S.P., Li, X.L., Cao, M.L., Xie, J.Y., Chen, P., and Huang, R.H. 2000. Indentification of venom proteins of spider *S. huwena* on two-dimensional electrophoresis gel by N-terminal microsequencing and mass spectrometric peptide mapping. *J. Protein Chem.* **19:** 225–229.

Lu, S.Y., Liang, S.P., and Gu, X.C. 1999. Three-dimentional structure of *Selenocosmia huwena* lectin-I from the venom of the spider *Selenocosmia huwena*. *J. Protein Chem.* **18:** 609–617.

Norton, R.S. and Pallaghy, P.K. 1998. The cystine knot structure of ion channel toxins and related polypeptides. *Toxicon* **36:** 1573–1583.

Omecinsky, D.O., Holub, K.E., Adams, M.E., and Reily, M.D. 1996. Three-dimensional structure analysis of μ-agatoxins: Further evidence for common motifs among neurotoxins with diverse ion channel specificities. *Biochemistry* **35:** 2836–2844.

Pallaghy, P.K., Nielsen, K.J., Craik, D.J., and Norton, R.S. 1994. A common structural motif incorporating a cystine knot and a triple-stranded β-sheet in toxic and inhibitory polypeptides. *Protein Sci.* **3:** 1833–1839.

Pallaghy, P.K., Alewood, D., Alewood, P.F., and Norton RS. 1997. Solution structure of robustoxin, the lethal neutotoxin form the funnel-web spider Atrax robustus. *FEBS Lett.* **419:** 191–196.

Qu, Y.X., Liang, S.P., Ding, J.Z., Liu, X.C., Zhang, R.J., and Gu, X.C. 1997. Proton nuclear magnetic resonance studies on huwentoxin-I from the venom of the spider *Selenocosmia huwena*: 2. Three-dimensional structure in solution. *J. Protein Chem.* **16:** 565–574.

Reily, M.D., Holub, K.E., Gray, W.R., Norris, T.M., and Adams, M.E. 1994. Structure-activity relationships for P-type calcium channel-selective ω-agatoxins. *Nat. Struct. Biol.* **1:** 853–856.

Reily, M.D., Thanabal, V., and Adams, M.E. 1995. The solution structure of ω-Aga-IVB, a P-type calcium channel antagonist from venom of the funnel web spider, *Agelenopsis aperta*. *J. Biomol. NMR* **5:** 122–132.

Shu, Q. and Liang, S.P. 1999. Purification and characterization of huwentoxin-II, a neurotoxic peptide from the venom of the Chinese bird spider *Selenocosmia huwena*. *J. Pept. Res.* **53:** 486–491.

Shu, Q., Huang, R.H., and Liang, S.P. 2001a. Assignment of disulfide bonds of Huwentoxin-II by Edman degradation sequencing and stepwise thiol modification. *Eur. J. Biochem.* **268:** 2301–2307.

Shu, Q., Lu, S.Y., Gu, X.C., and Liang, S.P. 2001b. Sequence-specific assignment of ^{1}H-NMR resonance and determination of the secondary structure of HWTX-II. *Acta Biochim. Biophys. Sinica.* **33:** 65–70.

Szeto, T.H., Birinyi-Strachan, L.C., Smith, R., Connor, M., Christie, M.J., King, G.F., and Nicholson, G.M. 2000. Isolation and pharmacological characterization of delta-atracotoxin-Hv1b, a vertebrate-selective sodium channel toxin. *FEBS Lett.* **470:** 293–299.

Takahashi, H., Kim, J.I., Min, H.J., Sato, K., Swartz, K.J., and Shimada, I. 2000. Solution structure of hanatoxin1, a gating modifier of voltage-dependent K(+) channels: Common surface features of gating modifier toxins. *J. Mol. Biol.* **297:** 771–780.

Wang, X., Connor, M., Smith, R., Maciejewski, M.W., Howden, M.E.H., Nicholson, G.M., Christie, M.J., and King, G.F. 2000. Discovery and characterization of a family of insecticidal neurotoxins with a rare vicinal disulfide bridge. *Nat. Struct. Biol.* **7:** 505–513.

Wüthrich, K. 1986. *NMR of proteins and nucleic acids.* John Wiley, New York.

Yu, H., Rosen, M.K., Saccomano, N.A., Phillips, D., Volkmann, R.A., and Schreiber, S.L. 1993. Sequential assignment and structure determination of spider toxin ω-Aga-IVB. *Biochemistry* **32:** 13123–13129.